https://doi.org/10.5194/egusphere-2026-3905
Preprint. Discussion started: 17 August 2026

Fusing geostationary satellite cloud properties with signal attenuation from microwave links for rain detection

Taoufiq Shit[1], Martin Fencl[1], Christian Chwala[2], and Vojtěch Bareš[1]

[1]Czech Technical University in Prague, Faculty of Civil Engineering, Prague, Czech Republic
[2]Institute of Meteorology and Climate Research (IMK-IFU), Karlsruhe Institute of Technology, Garmisch-Partenkirchen, Germany

Correspondence: Taoufiq Shit (taoufiq.shit@fsv.cvut.cz)

Abstract. Rain detection is hydrologically relevant because it defines rainfall occurrence, event onset, dry spell duration, and the spatial footprint of rainfall. These characteristics are inherently difficult to capture accurately at sub-hourly scale, and the challenge is amplified in data-scarce regions where conventional observations are sparse, making rainfall timing and volume quantification unreliable. Observations from geostationary satellites and networks of commercial microwave links (CMLs) can help in this regard. This paper proposes a convolutional neural network (CNN) algorithm that combines CML total loss with two SEVIRI products at 15 min resolution: Cloud Physical Properties (CPP) and Precipitating Cloud (PC). The satellite products are mapped to each CML path and used with the CML total loss time series. The models are evaluated on independent CML datasets from Germany and Czech Republic with 3692 and 1445 CMLs, respectively. The novelty of the proposed framework lies in integrating CML total-loss time windows with path-matched CPP and PC information within a single CNN, evaluating how the resulting wet–dry classification affects the rainfall volume retained, missed, or falsely attributed to dry periods, and testing transfer between two independent national CML networks.

In general, models combining SEVIRI and CML information outperform the CML-only model and fixed-threshold SEVIRI benchmark. The CML-only model retains 53 % of the reference rainfall volume and misses 35 %. Adding SEVIRI information reduces missed rainfall: the model using total loss and PC retains 81 %, the model using total loss and CPP retains 85 %, and the model using total loss with both CPP and PC retains 89 %, with only 8 % missed rainfall. The increase in retained rainfall volume with both CPP and PC directly improves rainfall accumulation for subsequent hydrological analyses. The gain is strongest around 1.0–2.5 mm h^{-1}, while falsely detected rainfall remains low. Satellite-informed models also show more stable performance when transferred between Germany and the Czech Republic.

1 Introduction

Reliable information on rainfall occurrence, onset, and dry intervals is important for hydrological modelling, urban flood forecasting, and water resources management. In urban catchments, fast runoff processes require rainfall information at high spatial and temporal resolution, making the timing and location of rainfall particularly important (Bruni et al., 2015). Errors in distinguishing rainy from dry conditions are also an important source of uncertainty in regional and global precipitation products, and can propagate into hydrological and land surface modelling applications (Dong et al., 2020). Such errors can

https://doi.org/10.5194/egusphere-2026-3905
Preprint. Discussion started: 17 August 2026

distort the estimated amount, timing, and duration of rainfall events, even when accumulated rainfall totals appear reasonable. The hydrological relevance of these errors has also been demonstrated in modelling studies: Tobin and Bennett (2010) reported improved daily streamflow simulations after correcting rainfall-detection errors, Miao et al. (2024) found hydrological model performance to be particularly sensitive to the correct detection of moderate rainfall, and Bárdossy and Anwar (2023) showed that underestimated rainfall volume can lead to underestimated peak flows. For this reason, precipitation products are commonly evaluated not only using rainfall amount errors, but also using categorical metrics that quantify missed rainfall and false detections (Zambrano-Bigiarini et al., 2017).

However, observing where and when rainfall starts, persists, and stops remains challenging at the spatial and temporal scales required by many hydrological applications. Rain gauges provide accurate local measurements but represent only conditions at a single point and are often sparse or absent in many regions. Weather radars provide spatially distributed rainfall information, but radar coverage is incomplete in many regions and radar estimates are affected by uncertainties related to beam blockage, ground clutter, range effects, and the need for calibration or adjustment with ground observations (Rombeek et al., 2025; Overeem et al., 2024). These limitations motivate the use of complementary observations that can improve rainfall occurrence information where conventional monitoring networks are sparse, uncertain, or unavailable.

Commercial microwave links (CMLs) and geostationary satellite observations are two promising complementary data sources. CMLs are part of existing cellular telecommunication networks and measure the attenuation of microwave signals between transmitting and receiving antennas. Because rainfall attenuates these signals, CMLs can provide path-integrated information on rainfall occurrence and intensity (Messer et al., 2006; Chwala et al., 2012; Overeem et al., 2013). Geostationary satellites, such as MSG SEVIRI, provide repeated observations of cloud and precipitation properties every 15 min over large domains. Their complementarity is especially relevant for data-poor regions, where rain gauge networks are sparse and radar coverage is limited or absent (Bonkoungou et al., 2025; Blettner et al., 2024).

For rainfall monitoring from CMLs, wet–dry classification is a critical step because it determines how the observed signal is separated into background variability and attenuation caused by rainfall. If dry periods are incorrectly classified as rain, non-rain signal fluctuations can be interpreted as rainfall. If rainy periods are classified as dry, rainfall-induced attenuation can be absorbed into the dry-weather baseline and partly removed from the retrieval. This makes rain and dry classification important both as a rain detection problem and as a preprocessing step for CML rainfall estimation. Improved classification therefore feeds directly into CML rainfall products used for hydrological modelling, urban flood applications, and rainfall monitoring in regions with limited conventional observations.

This classification problem is difficult because CML signals are affected not only by rainfall, but also by electromagnetic noise, temperature effects, hardware behaviour, signal quantisation, and other attenuation changes that are unrelated to rain (Polz et al., 2020; Blettner et al., 2023; Graf et al., 2024). These effects can make dry periods appear rain-like, especially for noisy or unstable links. They can also reduce the ability of a model trained on one CML network to perform well on another network, because link length, frequency, hardware properties, signal processing, and baseline stability can differ between networks. This transferability issue is particularly important for practical applications in data-poor regions, where long local reference records may not be available for retraining or calibration.

https://doi.org/10.5194/egusphere-2026-3905
Preprint. Discussion started: 17 August 2026

Satellite information can help reduce this ambiguity by adding independent atmospheric context. In particular, SEVIRI Cloud Physical Properties (CPP) describe cloud properties such as cloud water path, optical thickness, phase, and particle size, while the Precipitating Cloud product (PC) provides a satellite-based estimate of the probability of precipitation. These products can help distinguish attenuation associated with rainfall from non-rain CML signal variability and can reduce missed rainfall events or false detections. This fusion perspective is also relevant for rainfall applications that use satellite data, because CMLs provide near-surface information that can complement cloud and precipitation information from geostationary satellites.

Existing approaches have often used satellite information through fixed rules or as an external correction to a signal-based classifier, rather than learning the CML and satellite information jointly. Previous studies illustrate these different approaches. van het Schip et al. (2017) used predefined PC and CPP criteria, Kumah et al. (2021) used daytime MSG imagery to estimate rain area and wet path length for a single CML in Kenya, and Graf et al. (2024) combined separate CML and SEVIRI classifications through predefined decision rules. Machine learning studies on CML wet–dry classification have also used a range of models, including recurrent or LSTM based approaches, convolutional neural networks, feedforward neural networks or multilayer perceptrons, and other supervised classifiers (Habi and Messer, 2018; Polz et al., 2020; Pudashine et al., 2020; Kamtchoum et al., 2022; Blettner et al., 2023; Øydvin et al., 2024). However, most evaluations have relied on temporal splits, random splits, testing within one CML network, or experiments based on limited CML samples, whereas transfer between independent national CML networks with different link characteristics and data quality has received less attention.

Three questions therefore remain open. First, it is not yet clear how much direct CML–SEVIRI learning improves rain detection compared with a CML-only CNN and with existing benchmark approaches. Second, it remains unclear whether satellite information improves the hydrologically relevant behaviour of CML rain detection, especially during noisy dry periods and observed rainfall events. This is important because false rain detections can contaminate CML rainfall products, while missed rainfall can reduce event totals and distort rainfall timing. Third, the transferability of rain detection models between independent telecommunication networks remains insufficiently tested.

This study addresses these questions by developing a convolutional neural network (CNN) framework that combines CML total loss time windows with SEVIRI CPP and PC products for rain detection. The novelty of this work is threefold. First, SEVIRI CPP and PC products are integrated directly into the CNN together with CML total loss. Second, the analysis goes beyond standard classification scores by examining the rainfall volume retained, missed, and falsely assigned to dry periods. This shows whether the satellite inputs also reduce false wet responses and preserve hydrologically relevant rainfall. Third, the evaluation tests spatial generalisation and transfer between two independent national CML networks in Germany and the Czech Republic. This allows us to assess whether satellite information reduces dependence on link-specific CML signal behaviour and improves performance on new networks. The central hypothesis is therefore that joint learning from CML total loss and SEVIRI products reduces dry-period rain probabilities, preserves rainfall volume, and improves transfer compared with state-of-the-art methods and a CML-only CNN.

https://doi.org/10.5194/egusphere-2026-3905
Preprint. Discussion started: 17 August 2026

2 Material

2.1 Rainfall characteristics

To characterise the rainfall conditions during the June 2021 study period, the rainfall data were analysed in both domains. The study period is strongly dominated by dry conditions, with dry fractions of 94.20 % in Germany and 94.78 % in Czech Republic. The corresponding wet fractions are 5.80 % and 5.22 %, respectively. This strong imbalance is typical for CML wet–dry classification and motivates the use of skill scores that are less sensitive to class imbalance.

Although wet periods are relatively rare, the study period contains a substantial rainfall volume in both domains. Light rainfall is the most frequent wet class: rain rates below or equal to 1.0 mm h^{-1} account for 51.86 % of wet samples in Germany and 46.54 % in Czech Republic. However, these light rainfall samples contribute only 8.91 % and 6.36 % of the total rainfall volume, respectively.

Most of the rainfall volume is produced by moderate and heavy rainfall. Together, the moderate and heavy classes contribute 75.07 % of the total rainfall volume in Germany and 82.49 % in Czech Republic. The heavy rainfall class alone contributes 28.69 % and 28.10 % of the rainfall volume, despite representing only 3.64 % and 4.82 % of wet samples. The study period therefore contains both frequent rainfall of low intensity and rainfall with a high contribution to the total volume. This provides a useful test case for evaluating whether the models can detect light rainfall while also preserving sensitivity to stronger rainfall events.

2.2 Commercial microwave link observations

2.2.1 Czech Republic.

The primary dataset comprises CML measurements from the T-Mobile Czech Republic network collected during June 2021. It contains one-minute resolution records of transmitted and received signal power for approximately 2 887 links (5 774 sublinks), with missing values below 0.1 % for both quantities. Operating frequencies range from approximately 7.45 GHz to 85.75 GHz and path lengths from approximately 0.03 km to 36 km (Fig. 1a). Due to the spatial coverage of the RADKLIM–YW radar product, 1 445 links were retained for the final analysis. The spatial distribution of the network is shown in Fig. 2b.

2.2.2 Germany.

To assess geographic transferability, we use an independent German CML dataset covering the same period (June 2021), comprising approximately 3 692 links (Blettner et al., 2023). Operating frequencies span approximately 10 GHz to 38 GHz and path lengths range from approximately 0.5 km to 35 km (Fig. 1b). The spatial distribution is shown in Fig. 2a. The German network operates across a narrower frequency range than the Czech dataset, with most links concentrated below 40 GHz, reflecting different regulatory environments and deployment histories.

https://doi.org/10.5194/egusphere-2026-3905
Preprint. Discussion started: 17 August 2026

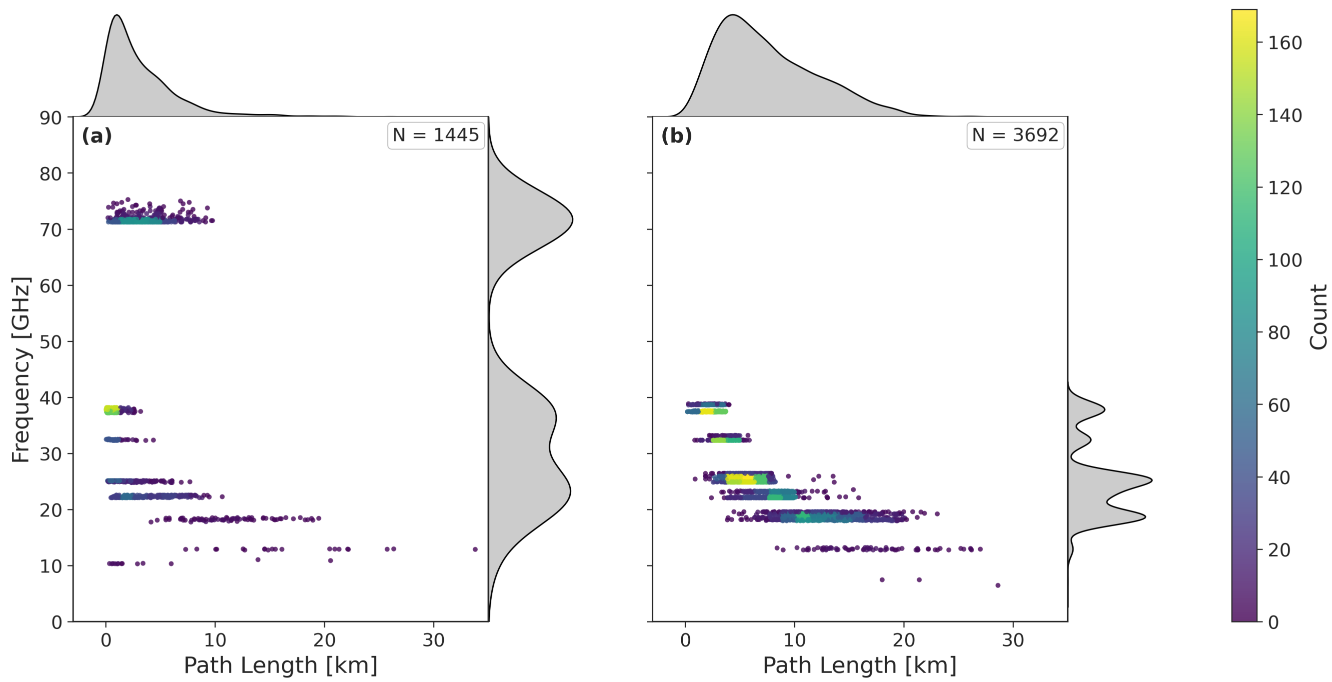

Figure 1. Joint distribution of CML path length and operating frequency for (a) the Czech Republic and (b) Germany. The Czech network includes links operating at frequencies up to approximately 80 GHz, whereas the German dataset is concentrated below 40 GHz.

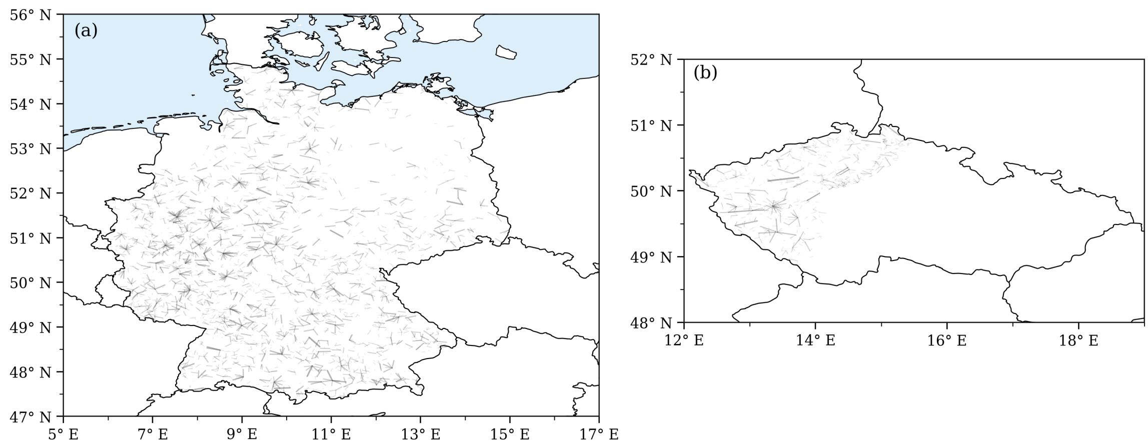

Figure 2. Spatial distribution of CMLs across (a) Germany and (b) the Czech Republic. Country boundaries are from Natural Earth public domain map data and were plotted using Cartopy.

https://doi.org/10.5194/egusphere-2026-3905
Preprint. Discussion started: 17 August 2026

2.3 Satellite cloud products from MSG SEVIRI

The satellite data used in this study are derived from the Spinning Enhanced Visible and Infrared Imager (SEVIRI) on board Meteosat Second Generation (MSG). SEVIRI is a passive imager with 12 spectral channels from the visible to the thermal infrared, providing a spatial sampling of approximately 3 km at the subsatellite point and a full disk scan every 15 min (EUMETSAT, 2017). Two SEVIRI-derived products are used in this study: Cloud Physical Properties (CPP) and Precipitating Clouds (PC).

2.3.1 Cloud Physical Properties (CPP).

The CPP product is part of the CLAAS-3 dataset (Meirink et al., 2022) and provides cloud thermodynamic and microphysical properties retrieved from SEVIRI observations. In this study, the CPP input set includes cloud water path (`cwp`), cloud optical thickness (`cot`), cloud droplet number concentration (`cdnc`), cloud particle effective radius (`cre`), cloud phase (`cph`), and cloud geometrical thickness (`cgt`).

These variables describe different aspects of the cloud field that are relevant for precipitation formation. Cloud water path represents the vertically integrated cloud water content, cloud optical thickness describes the optical depth of the cloud, and cloud droplet number concentration provides information on the concentration of liquid cloud droplets. Cloud particle effective radius describes the characteristic size of cloud droplets or ice particles, cloud phase indicates whether the cloud is liquid, mixed-phase, or ice, and cloud geometrical thickness provides information on the vertical depth of liquid clouds.

The availability of the CPP variables differs between day and night. Cloud phase (`cph`) is available during both daytime and nighttime because it is based on thermal infrared measurements. In contrast, cloud water path (`cwp`), cloud optical thickness (`cot`), cloud droplet number concentration (`cdnc`), cloud particle effective radius (`cre`), and cloud geometrical thickness (`cgt`) rely on reflected solar radiation and are therefore available only during daytime.

2.3.2 Precipitating Clouds (PC).

The Precipitating Clouds (PC) product from the NWC SAF provides a per-pixel estimate of precipitation likelihood based on regression models using multispectral SEVIRI information (Graf et al., 2024). In contrast to the CPP variables, which describe cloud physical properties, PC is a direct satellite-based indicator of whether a cloud scene is likely to produce precipitation. The product provides precipitation probability rather than rain rate, and is therefore used in this study as an atmospheric-context variable for wet–dry classification.

Separate daytime and nighttime versions exist due to the reduced number of channels available after sunset. During daytime, visible, near-infrared, and infrared SEVIRI information can be used, whereas the nighttime retrieval relies mainly on thermal infrared channels. PC is therefore available throughout the diurnal cycle, but the spectral information used by the algorithm differs between day and night.

https://doi.org/10.5194/egusphere-2026-3905
Preprint. Discussion started: 17 August 2026

2.4 Reference data: gauge-adjusted weather radar

As reference for the wet–dry classification, we use the RADKLIM–YW product of the German Meteorological Service (DWD). RADKLIM–YW is the 5 min precipitation-rate product of the DWD radar-based precipitation climatology. The YW fields are quasi gauge-adjusted using the RADKLIM–RW product and are provided on a 1 km × 1 km polar-stereographic grid (Bartels et al., 2004; Winterrath et al., 2012, 2018). The product covers Germany and extends partly into Czech Republic near the German border, which allows its use for the subset of Czech CMLs located inside the available radar domain.

The 5 min temporal resolution of RADKLIM–YW is important for this study because it provides sub-hourly rainfall occurrence information and can be aggregated to the 15 min SEVIRI time step used by the CNN inputs. In this study, RADKLIM–YW is used only as reference information for deriving wet–dry labels and for evaluating rainfall-volume contributions. The path-based extraction of RADKLIM–YW along CMLs and its aggregation from 5 min to 15 min resolution are described in the data preprocessing section.

3 Methods

3.1 Data preprocessing

3.1.1 CML signal processing.

Before training the CNN, the raw 1 min CML time series undergo several preprocessing steps. For each sublink of every CML, the total path loss (TL) is computed by subtracting the received signal level from the transmitted signal level for each sublink (TL1 and TL2). Links that were not in operation or that contained long periods with missing or invalid measurements are removed from the dataset. CMLs located outside the RADKLIM–YW coverage area are also excluded due to the lack of reference data.

Within each remaining TL time series, short gaps of up to 5 minutes are linearly interpolated following Graf et al. (2024). These gaps are short relative to the characteristic temporal variability of rainfall in the study region, making it unlikely that complete rain events are missed.

To account for slow signal drifts, each time step is normalised by subtracting the median of the preceding 72 hours. Among several normalisation strategies evaluated by Polz et al. (2020), this approach yielded the best model performance. After normalisation, the CML data are resampled using the mean to 15 min temporal resolution to match the satellite observations.

3.1.2 CML-path extraction of SEVIRI and RADKLIM–YW data.

SEVIRI and RADKLIM–YW data are provided on different grids and projections, but both were extracted along CML paths using the same length-weighted principle. For each product, the CML endpoints were first transformed to the corresponding data projection. The straight line connecting the two endpoints was then intersected with the product grid, and all crossed pixels or grid cells were identified. Each crossed cell was weighted by the fraction of the CML path length inside that cell.

https://doi.org/10.5194/egusphere-2026-3905
Preprint. Discussion started: 17 August 2026

For SEVIRI, the Precipitating Cloud probability (PC) and Cloud Physical Properties (CPP) were extracted for each 15 min time slot following Graf et al. (2024). Continuous variables were averaged along the CML path using the length-based weights. For cloud phase, the most frequent class along the path and the corresponding class fractions were stored. Daytime-only CPP variables were set to zero during nighttime after the StandardScaler was fitted on daytime values, while cloud phase remained available throughout.

For RADKLIM–YW, 5 min rain-rate fields were extracted along the same CML paths following Graf et al. (2020) and then aggregated to 15 min resolution. A threshold of 0.1 mm,h^{-1} was applied to obtain the binary wet–dry reference, with all values below this threshold classified as dry. This threshold is consistent with previous CML studies (Graf et al., 2020, 2024) and represents the lower bound of reliably detectable rainfall for most CML configurations.

3.2 CNN architecture and model configurations

The wet–dry classifier is based on the one-dimensional convolutional neural network proposed by Polz et al. (2020). The original model uses the CML signal from two sublinks as input and is also available as a baseline classifier in the open source `pycomlink` package, which provides Python tools for CML data processing and includes several wet–dry classification methods (Chwala et al., 2026). In this study, the same general CNN concept is used, but the input is extended with SEVIRI cloud and precipitation variables. The architecture and the tested input configurations are shown in Fig. 3.

Each input sample covers one hour and is sampled at 15 min resolution, resulting in four time steps per sample. For each CML, the input contains the two total loss time series from the two sublinks and, depending on the model configuration, additional SEVIRI variables extracted along the CML path. The SEVIRI CPP and PC variables are first averaged along the CML path so that they represent the same path scale as the CML observation. The CNN then maps the combined input sequence to one sigmoid output, interpreted as the probability that the CML path is wet at the target time step.

All CNN configurations use the same architecture, input window, and reference labels. They differ only in the input feature set (Table 1). The `CNN-TL` model uses only the CML total loss and serves as the baseline. The other configurations add SEVIRI CPP variables, the SEVIRI precipitating cloud probability (PC), or both. Keeping the architecture fixed ensures that differences in performance are linked to the input information rather than to changes in the neural network design.

https://doi.org/10.5194/egusphere-2026-3905
Preprint. Discussion started: 17 August 2026

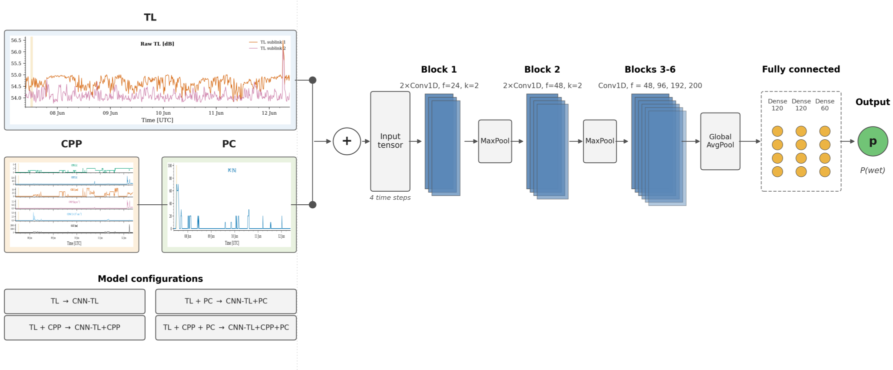

Figure 3. Architecture of the 1D CNN used for wet–dry classification. The left part shows the CML and SEVIRI inputs and the four tested model configurations. The right part shows the convolutional feature extraction, global average pooling, fully connected layers, and final sigmoid output used to estimate the wet probability.

Table 1. CNN model configurations used for wet–dry classification.

Configuration	Input features	Availability	Purpose
`CNN-TL`	TL (two sublinks)	TL: all times	CML-only baseline used to quantify the added value of satellite information.
`CNN-TL+CPP`	TL + CPP (`cwp`, `cot`, `cdnc`, `cre`, `cph`, `cgt`)	TL,`cph`: day–night; other: day only	Tests whether cloud physical information helps distinguish rainfall-induced attenuation from non-rain TL variability.
`CNN-TL+PC`	TL + PC (`pc`)	TL, PC: day–night	Tests the added value of the SEVIRI precipitating cloud probability product as direct CNN input.
`CNN-TL+CPP+PC`	TL + CPP (`cwp`, `cot`, `cdnc`, `cre`, `cph`, `cgt`) + PC (`pc`)	TL, PC, `cph`: day–night; other: day only	Tests whether CPP and PC provide complementary information.

3.3 Benchmark methods

Two established wet–dry detection approaches are used as benchmarks. The first is the rolling standard deviation (RSTD) method, which detects wet periods based on increased short term variability in the CML signal loss (Schleiss and Berne, 2010). For each sublink, the rolling standard deviation of the path loss signal is computed over a 60 min window. A time step is classified as wet when the RSTD of either sublink exceeds a link specific threshold. In the RSTD–Q80 configuration evaluated here, this threshold is defined per link as the 80th percentile of the 60 min rolling standard deviation computed over the full study period, multiplied by a scaling factor of 1.12 following Graf et al. (2020). Because RSTD is inherently a binary classifier,

https://doi.org/10.5194/egusphere-2026-3905
Preprint. Discussion started: 17 August 2026

it does not produce continuous probability scores. To enable consistent comparison with probabilistic CNN models across varying discrimination thresholds, we use the maximum RSTD value across both sublinks as a continuous decision variable and construct ROC curves by sweeping detection thresholds over this signal.

The second benchmark, CNN–WET82–PC, combines a CNN trained on total loss with decision rules derived from the SEVIRI Precipitating Cloud product, which takes the wet/dry decision of a CML-only CNN and overrides it using the SEVIRI PC product: very low PC forces the decision to dry, very high PC forces it to wet, and intermediate PC values leave the CNN decision unchanged; following Graf et al. (2024). To maintain comparability within the ROC framework, the continuous CNN probability is retained as the base signal, while deterministic constraints derived from PC thresholds are mapped to probabilities of zero or one.

3.4 Training and experimental design

3.4.1 Spatial split.

The Czech and German CML datasets were divided into training, validation, and test subsets using a spatial holdout split. Fig. 4 shows the spatial distribution of the selected CMLs. The split was not random, but was designed to evaluate spatial generalisation to links with different local signal behaviour. Training links were selected from the central part of each domain, while validation and test links were selected from the outer regions. A minimum distance of 20 km was used between any two of the three groups to reduce spatial dependence; therefore, no training link was used in the validation process, and no training or validation link was used in the final evaluation. Validation links were used exclusively for early stopping and model checkpointing, and test links were used exclusively for the final reported metrics, so the same data were never used for both selecting and evaluating the model. Many previous CML wet–dry classification studies have used temporal splits, random splits, cross validation within the same CML network, or experiments based on a limited number of CMLs (Habi and Messer, 2018; Pudashine et al., 2020; Polz et al., 2020; Kamtchoum et al., 2022). These approaches are appropriate for estimating model performance when training and validation data come from similar link conditions. However, they are less strict for evaluating transferability. For the Czech dataset, this split gave 469 training links, 144 validation links, and 468 test links. The remaining links were removed because they were located inside the 20 km buffer zone between the three groups. Similarly, for the German dataset, the split gave 1 366 training links, 390 validation links, and 1 508 test links, with the remaining links removed for the same reason.

3.4.2 Class balancing and model training.

Dry periods occur much more often than wet periods. Therefore, class balancing was applied only during model training. For each training setup, dry samples in the train set were downsampled to match the number of wet samples, resulting in a 50:50 wet–dry ratio during training. The validation and test sets were not balanced and kept their original class distribution. Consequently, the validation and test sets preserve the natural class imbalance of the CML datasets. The final reported scores are computed on the held-out test links.

https://doi.org/10.5194/egusphere-2026-3905
Preprint. Discussion started: 17 August 2026

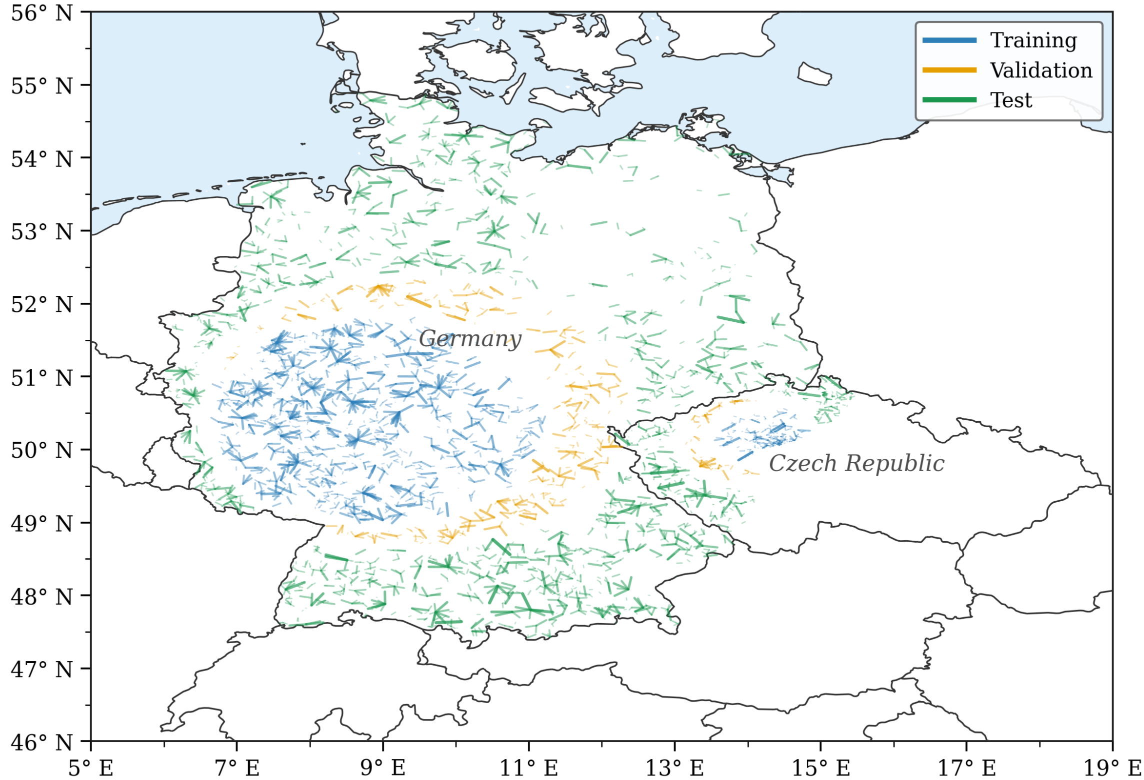

Figure 4. Spatial split of the CML networks. Training links are located in the central domain, while validation and test links are held out in the outer regions with a minimum 20 km separation. Country boundaries are from Natural Earth public domain map data and were plotted using Cartopy.

All models used the same preprocessing, architecture, and hyperparameters. The loss function was binary cross entropy. The optimiser was stochastic gradient descent with Nesterov momentum, using a learning rate of 0.005, momentum of 0.90, and weight decay of 10^{-3}. Training was run for up to 100 epochs with a batch size of 32. The final model weights were selected from the epoch that maximised wet-period recall on the spatially independent validation links, which were held at least 20 km away from the train links and were not used for model fitting. The selected model was then evaluated on the held-out test links, which were spatially independent from both the train and validation links. All experiments were run with the same random seed (e.g., 42) using TensorFlow/Keras on a single NVIDIA H100 NVL GPU.

3.4.3 Training setups.

The experiments were designed to test transfer between the German and Czech CML networks. For each test domain, the test links were kept fixed and only the training domain was changed. This design makes it possible to interpret differences in performance mainly as the effect of the training data, rather than as changes caused by different test samples.

https://doi.org/10.5194/egusphere-2026-3905
Preprint. Discussion started: 17 August 2026

In the same-domain setups (`DE/DE` and `CZ/CZ`), the model was trained and tested on spatially separated links from the same country. In the cross-domain setups (`CZ/DE` and `DE/CZ`), the model was trained on one country and tested on the other. The mixed setup combines German and Czech training links from the spatial split, thereby increasing the diversity of the training data while preserving the same holdout design. Validation links were taken from the corresponding training domain and used for model selection. Table 2 summarises the main setups.

The mixed setup was used as the main setup for the ROC analysis and the rainfall contribution analysis because it provides the most diverse training set while preserving the spatial holdout design. The cross-domain setups were used to assess whether the proposed models remain effective when applied to a CML network not used during training.

In addition to the main setups listed in Table 2, two single-source all-link transfer tests were included in the Supplement: `CZ-all/DE` and `DE-all/CZ`. These tests evaluate whether using more links from one source country changes the transfer trends. For these supplementary tests only, the internal training–validation split within the source country was random rather than spatial, because the final test links belonged to the other country. The results are reported in Sect. S1.2 and Fig. S2 of the Supplement.

Table 2. Training, validation, and test setups. For each country, the links are split into three spatially separated sets: training, validation, and test. Validation is used for early stopping and checkpoint selection, and test links are used only for the final reported results.

Setup	Training	Validation	Test
`DE/DE`	DE ($N_{\mathrm{DE}}^{\mathrm{train}} = 1366$)	DE ($N_{\mathrm{DE}}^{\mathrm{val}} = 390$)	DE ($N_{\mathrm{DE}}^{\mathrm{test}} = 1508$)
`CZ/CZ`	CZ ($N_{\mathrm{CZ}}^{\mathrm{train}} = 469$)	CZ ($N_{\mathrm{CZ}}^{\mathrm{val}} = 144$)	CZ ($N_{\mathrm{CZ}}^{\mathrm{test}} = 468$)
`CZ/DE`	CZ ($N_{\mathrm{CZ}}^{\mathrm{train}} = 469$)	CZ ($N_{\mathrm{CZ}}^{\mathrm{val}} = 144$)	DE ($N_{\mathrm{DE}}^{\mathrm{test}} = 1508$)
`DE/CZ`	DE ($N_{\mathrm{DE}}^{\mathrm{train}} = 1366$)	DE ($N_{\mathrm{DE}}^{\mathrm{val}} = 390$)	CZ ($N_{\mathrm{CZ}}^{\mathrm{test}} = 468$)
`Mixed`	DE + CZ ($1366 + 469 = 1835$)	DE + CZ ($390 + 144 = 534$)	DE + CZ ($1508 + 468 = 1976$)

3.5 Evaluation

3.5.1 Reference labels and metrics.

Radar rainfall estimates at 15 min resolution were used as reference data. A time step was classified as wet when the path-averaged radar rain rate exceeded 0.1 $\mathrm{mm\,h^{-1}}$, consistent with previous CML studies (Graf et al., 2020, 2024). For the CNN models, wet–dry labels were obtained by applying a probability threshold of 0.8 to the model output. This choice is appropriate for the strongly imbalanced wet–dry classification problem, where a lower threshold can increase false wet detections. A similar use of a high decision threshold for CNN based CML wet–dry classification was also reported by Polz et al. (2020). The same threshold was then applied consistently to all CNN configurations in the test and transfer experiments. Based on these criteria, a confusion matrix was constructed by comparing the predicted and reference classes.

https://doi.org/10.5194/egusphere-2026-3905
Preprint. Discussion started: 17 August 2026

Table 3. Confusion matrix notation.

	Predicted Wet	**Predicted Dry**
Actual Wet	TP	FN
Actual Dry	FP	TN

Here, TP denotes correctly identified wet time steps, and TN denotes correctly identified dry time steps. FP corresponds to dry periods incorrectly classified as wet, while FN corresponds to missed rainfall events. From the confusion matrix, the true-positive rate (TPR) and false-positive rate (FPR) were defined as

$$\mathrm{TPR} = \frac{TP}{TP+FN} \tag{1}$$

$$\mathrm{FPR} = \frac{FP}{FP+TN} \tag{2}$$

Here, TPR measures the fraction of radar-detected wet time steps correctly identified as wet, while FPR measures the fraction of dry time steps incorrectly classified as wet.

The Matthews Correlation Coefficient (MCC) was used as the primary metric. MCC accounts for all four elements of the confusion matrix and remains informative under strongly imbalanced class distributions:

$$\mathrm{MCC} = \frac{TP \times TN - FP \times FN}{\sqrt{(TP+FP)(TP+FN)(TN+FP)(TN+FN)}}. \tag{3}$$

MCC ranges from -1 to $+1$, where -1 indicates complete disagreement, $+1$ indicates perfect classification, and 0 indicates no skill.

Receiver operating characteristic (ROC) curves and the area under the ROC curve (AUC) were used as complementary threshold-independent metrics. The ROC curve describes the trade-off between FPR and TPR as the classification threshold τ varies from 0 to 1 (Fawcett, 2006). The diagonal in ROC space represents random guessing, whereas the point $(0,1)$ corresponds to a perfect classifier. The AUC is defined as

$$\mathrm{AUC} = \int_0^1 \mathrm{TPR}(\mathrm{FPR})\, d\mathrm{FPR}. \tag{4}$$

The AUC ranges from 0 to 1. An AUC of 0.5 indicates no discrimination skill, corresponding to random guessing, while an AUC of 1 indicates perfect separation between wet and dry time steps. In this study, ROC curves and AUC values were used to compare the proposed CNN configurations and Benchmark methods across all possible thresholds.

https://doi.org/10.5194/egusphere-2026-3905
Preprint. Discussion started: 17 August 2026

All reported TPR, FPR, MCC, ROC curves, and AUC values were computed on the spatially independent test links defined in Sect. 3.4. These links were not used during model fitting or model selection, and their original wet–dry class distribution was preserved during evaluation.

3.5.2 Rainfall contribution analysis.

For the rainfall contribution analysis, CML rain rates were estimated only for time steps classified as wet by each CNN configuration. For each method, the wet mask was obtained by applying the same probability threshold of 0.8 to the CNN output. A baseline was then estimated from the five most recent dry time steps, and excess attenuation was computed relative to this baseline. A wet antenna attenuation correction based on Leijnse et al. (2008) was applied separately to both sublinks. The corrected rain attenuation was converted to rain rate using the ITU-R specific attenuation–rain-rate relation,

$$\gamma_R = kR^{\alpha}, \tag{5}$$

where γ_R is the specific attenuation in dB km^{-1} and R is the rain rate in mm h^{-1}. The coefficients k and α were derived from ITU-R Recommendation P.838-3 and depend on link frequency and polarisation (International Telecommunication Union, 2005).

The cumulative distribution function (CDF) analysis was used to assess how the wet–dry classification affects rainfall volume across intensity ranges. Rainfall intensity was divided using the following thresholds: dry conditions below 0.1 mm h^{-1}, light I rainfall from 0.1 to 1.0 mm h^{-1}, light II rainfall from 1.0 to 2.5 mm h^{-1}, moderate rainfall from 2.5 to 10.0 mm h^{-1}, and heavy rainfall above 10.0 mm h^{-1}.

In the CDF analysis, true positive (TP) and false negative (FN) rainfall contributions were calculated from the radar reference rain rate. False positive (FP) rainfall contributions were calculated from the CML-estimated rain rate, because these cases correspond to time steps classified as wet by the model but dry in the radar reference.

4 Results

This section first evaluates the rain detection skill of the tested methods under the mixed setup. It then examines whether the improved discrimination is partly related to lower rain probabilities during noisy dry periods. Next, it evaluates how the classification decisions affect rainfall volume across intensity classes. Finally, it assesses transfer between the Czech and German CML networks.

The mixed setup is used for the ROC analysis and the rainfall contribution analysis because it provides the most diverse training data while keeping the testing domains fixed. The transfer setups are then used to evaluate how the models perform when trained on one national network and applied to the other. Additional transfer setups using all available links from one country are reported in Sect. S1.2 and Fig. S2 of the Supplement.

https://doi.org/10.5194/egusphere-2026-3905
Preprint. Discussion started: 17 August 2026

4.1 Detection skill and link-level performance

Receiver operating characteristic (ROC) curves are used to evaluate the discrimination performance of the proposed and Benchmark methods for the Czech and German testing domains (Fig. 5). The models that use satellite information clearly outperform the CNN trained on total loss and the RSTD benchmark. The best performance is obtained by `CNN-TL+CPP` and `CNN-TL+CPP+PC`, but using only PC also gives a clear improvement over `CNN-TL`.

The shape of the ROC curves shows that the satellite enhanced models reach high true positive rates while keeping false positive rates low. For these models, the true positive rate already exceeds 0.60 at false positive rates below 0.05. This indicates improved separation between rainy and dry periods when satellite inputs are included.

The RSTD benchmark performs better than `CNN-TL` at higher false positive rates. This suggests that the CML-only CNN has difficulty detecting some marginal rainfall cases when only total loss is used. Adding CPP or PC reduces this limitation and improves the discrimination over most of the ROC curve.

The comparison between `CNN-TL+PC` and `CNN-WET82-PC` is also important. Both methods use the PC product, but they use it in different ways. `CNN-WET82-PC` applies PC through a rule based threshold step, whereas `CNN-TL+PC` learns PC together with CML total loss inside the CNN. The higher performance of `CNN-TL+PC` shows that PC is more useful when it is integrated directly into the model.

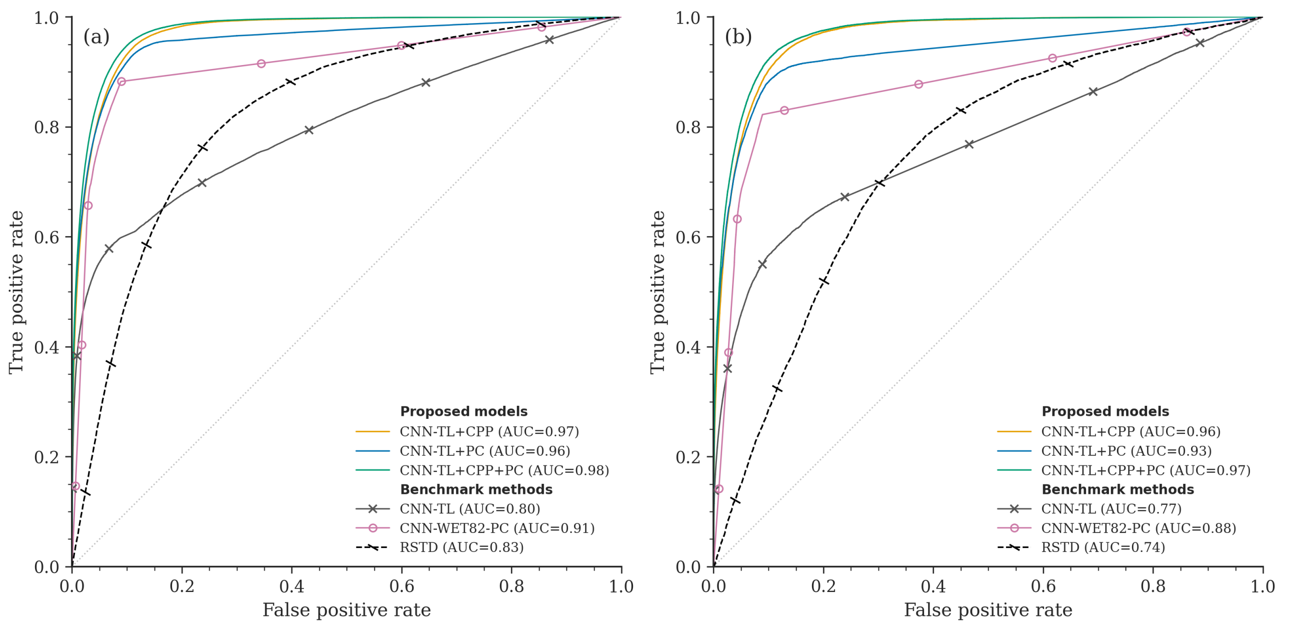

Figure 5. Receiver operating characteristic curves for wet–dry classification under the mixed setup. Panel (a) shows the German testing domain and panel (b) shows the Czech testing domain. The proposed CNN models that combine CML total loss with satellite inputs outperform the CML only CNN and the Benchmark methods in both domains.

https://doi.org/10.5194/egusphere-2026-3905
Preprint. Discussion started: 17 August 2026

This improvement can result from both a lower probability assigned to dry periods and a higher probability assigned to rainy periods. To examine one important part of this behaviour, we next focus on dry periods with strong CML signal variability. These cases are useful because they represent situations where a CML only model can confuse non rain signal fluctuations with rainfall.

4.2 Model response during noisy dry periods

The ROC analysis shows that the satellite based models reach higher detection rates while keeping false positive rates low. To examine one source of this improvement, Fig. 6 focuses on dry periods with strong CML signal variability. Here, high RSTD dry periods refer to radar dry samples ($RR \leq 0.1$ mm h^{-1}) where the rolling standard deviation of the total loss signal is within the upper 10 % of dry period values for each link. These periods represent a difficult case for a model trained only on total loss, because signal fluctuations unrelated to rainfall can still resemble rainfall attenuation.

Figure 6a illustrates this behaviour for two noisy links. During several high RSTD dry periods, the model trained only on total loss assigns elevated rain probabilities, in some cases close to or above the decision threshold. In contrast, the models that include SEVIRI information generally assign lower rain probabilities during the same dry intervals. This indicates that the satellite inputs reduce the dry period probability level and make the model more confident that these periods are dry.

Figure 6b shows that the same pattern is visible beyond the selected examples. Across high RSTD dry periods in the test data, the total loss only model has the highest rain probabilities and many values above the decision threshold. The satellite based models are shifted toward lower probabilities, with the strongest reduction obtained when both CPP and PC are used. This shows that the reduction in false wet response is not only a visual feature of selected links, but a general pattern under noisy dry conditions.

This behaviour suggests that the lower false positive rates observed in the ROC curves are partly attributable to reduced rain probabilities during high variability dry periods. The next section evaluates the complementary question of whether the same models also retain more observed rainfall volume.

https://doi.org/10.5194/egusphere-2026-3905
Preprint. Discussion started: 17 August 2026

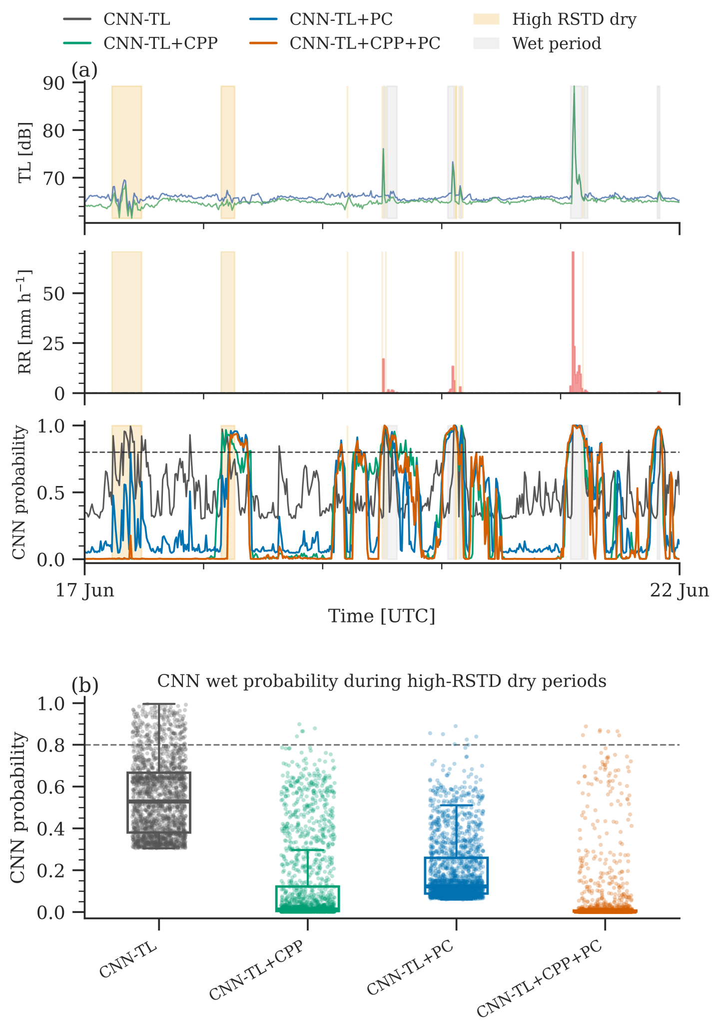

Figure 6. Model behaviour during noisy dry intervals. Panel (a) shows total path loss (TL), reference radar rain rate (RR), and CNN wet probabilities for a representative noisy link. Panel (b) shows the distribution of CNN wet probabilities during high-RSTD dry periods across test links. High RSTD dry periods are radar dry samples with rolling standard deviation in the upper 10 % of dry period values for each link.

4.3 Rainfall contribution across intensity classes

The previous subsection shows that satellite information partly reduces false detections by lowering rain probabilities during noisy dry periods. However, lower false detections are useful only if real rainfall is still retained. We therefore analyse how the classification decisions affect rainfall volume across intensity classes. For each model, the total rainfall contribution is divided into true positive (TP), false positive (FP), and false negative (FN) rainfall fractions (Fig. 7).

https://doi.org/10.5194/egusphere-2026-3905
Preprint. Discussion started: 17 August 2026

The model trained only on CML total loss retains a limited fraction of the reference rainfall volume. It captures 53 % of the total rainfall volume as true positive rainfall and misses 35 % as false negative rainfall (Fig. 7a). Adding satellite information strongly reduces the missed rainfall fraction. The model using total loss and PC captures 81 % of the reference rainfall volume, while the model using total loss and CPP captures 85 %. The model using total loss together with both CPP and PC gives the highest retained rainfall volume, with TP = 0.89 and FN = 0.08.

The reduction in missed rainfall is not accompanied by a large increase in false positive rainfall. The false positive rainfall fraction decreases from 0.12 for the total loss only model to 0.05 for the model using CPP, 0.04 for the model using PC, and 0.03 for the model using both CPP and PC. This shows that the satellite based models recover more reference rainfall volume without substantially increasing rainfall falsely assigned to dry periods.

The largest differences between the models occur above 1.0 mm h^{-1}. In the 1.0 to 2.5 mm h^{-1} range, the total loss only model already accumulates a clear false negative rainfall contribution, whereas the satellite based models begin to classify more of this rainfall as true positive. The same behaviour continues into the moderate and heavy rainfall ranges, where most of the retained rainfall volume is accumulated. In contrast, very light rainfall below 1.0 mm h^{-1} contributes little to the recovered rainfall volume for all models.

https://doi.org/10.5194/egusphere-2026-3905
Preprint. Discussion started: 17 August 2026

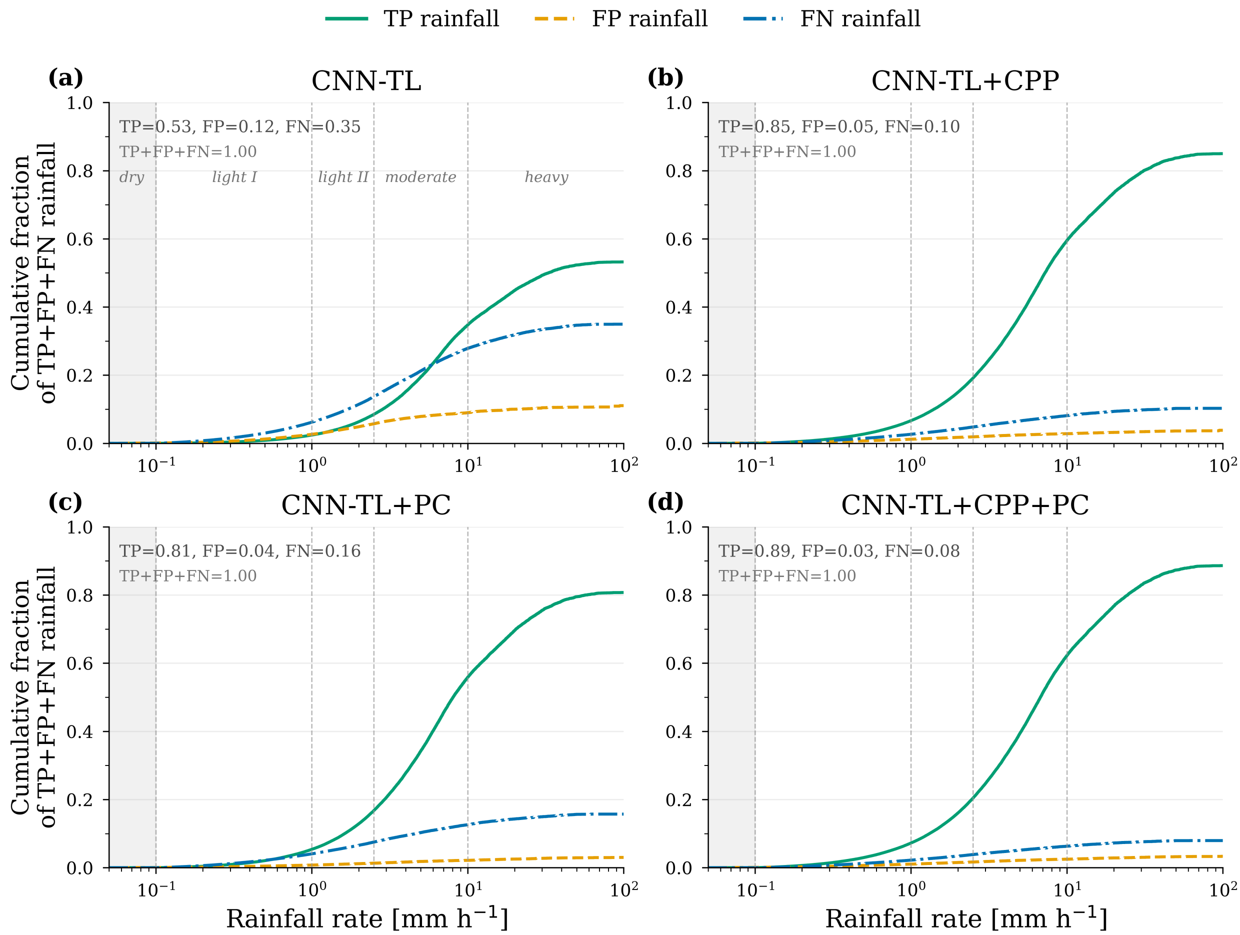

Figure 7. Cumulative rainfall contribution as a function of rain rate for all evaluated methods. Green, orange, and blue curves denote TP, FP, and FN rainfall contributions, respectively, normalized by the total TP+FP+FN rainfall contribution. The annotations report the hydrologically weighted TP, FP, and FN fractions.

4.4 Geographic transferability

The rainfall contribution analysis shows that the benefit of SEVIRI inputs is hydrologically meaningful, not only statistical. However, good performance within one dataset does not necessarily mean that the model will perform well on another dataset with different link properties, signal behaviour, and rainfall conditions. Therefore, the next step is to test whether this advantage remains when the models are applied to another CML network.

The transfer analysis uses the training setups defined in Table 2, including same country training, transfer between Germany and Czech Republic, and mixed training. Several satellite based configurations were tested in this study. For the transferability analysis shown in Fig. 8, we focus on `CNN-TL+PC` because it is the simplest satellite assisted configuration: it adds only one

https://doi.org/10.5194/egusphere-2026-3905
Preprint. Discussion started: 17 August 2026

satellite variable to the CML time series, while still providing competitive performance compared with the CPP based configurations shown in the previous analyses. The remaining transfer experiments are reported in the Supplement. The following section evaluates `CNN−TL+PC` against the CML only model `CNN−TL` across the same country, transfer, and mixed training setups.

The MCC distributions show that `CNN−TL+PC` is more stable across datasets than `CNN−TL`. In the German test domain, `CNN−TL+PC` consistently gives higher MCC distributions than `CNN−TL` for the same country, transfer, and mixed training setups. The improvement is especially clear when the model is trained on Czech links and evaluated on German links, where the CML only model shows a stronger drop in performance. This indicates that adding PC helps the CNN transfer better to an unseen CML network.

A similar pattern is observed in the Czech test domain. Both models perform better than in the German test case, but `CNN−TL+PC` still keeps higher and more compact MCC distributions than `CNN−TL`. This suggests that the satellite precipitation probability input improves not only the average detection skill, but also the consistency of the model across links.

The mixed training setup also performs well in both test domains. This is important because the model is trained using links from both Germany and Czech Republic, and then evaluated separately on each domain. The results show that mixed training does not favour only one dataset. Instead, it gives competitive MCC distributions for both Germany and Czech Republic. This suggests that combining training links from both domains helps the CNN learn more general rain and dry patterns than training on one dataset alone.

Additional configurations are reported in Sect. S1.2 and Fig. S2 of the Supplement. These include the CPP based models and the additional transfer setups in which all available links from one country are used for training. These experiments test whether using more input variables or more links from one country changes the same general trends. The results show that increasing model complexity or increasing the number of links from a single country does not automatically guarantee better transfer to the other dataset. The remaining gain from the mixed setup is therefore consistent with, although not isolated proof of, a benefit from training data diversity.

https://doi.org/10.5194/egusphere-2026-3905
Preprint. Discussion started: 17 August 2026

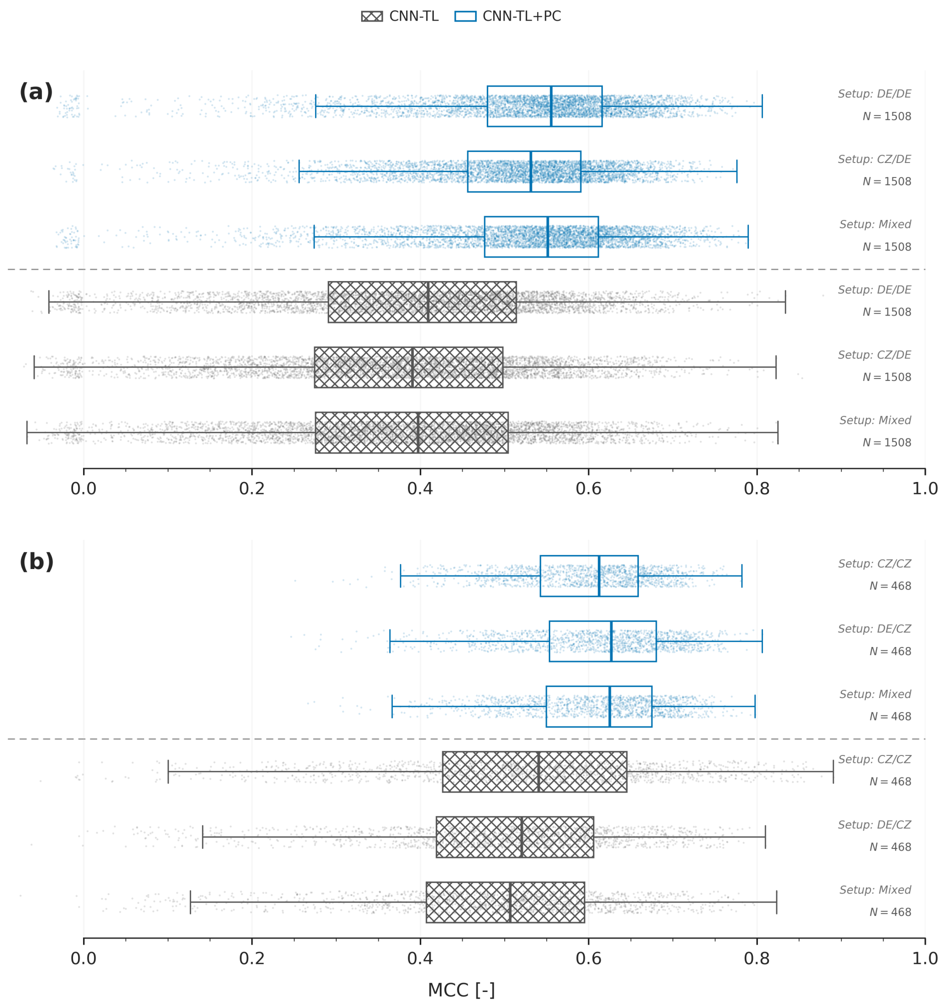

Figure 8. MCC distributions for the cross-domain transfer experiments. Panels (a) and (b) show the German and Czech Republic testing domains, respectively. With setup labels following the training/testing domain convention defined in Table 2.

5 Discussion

One difficulty in CML rain detection is that rainfall attenuation and non-rain signal variability can produce similar changes in total loss. The results suggest that SEVIRI information helps reduce this ambiguity by adding independent cloud and precipitation context. This interpretation provides the basis for discussing the added value of CML–SEVIRI fusion, its effect on rainfall volume, its behaviour during noisy dry periods, and its transfer between independent CML networks.

https://doi.org/10.5194/egusphere-2026-3905
Preprint. Discussion started: 17 August 2026

5.1 Added Value of CML–SEVIRI Fusion

CML total loss contains rainfall information, but also includes noise, baseline changes, wet antenna effects, and other signal changes unrelated to rain (Blettner et al., 2023). This makes wet–dry classification difficult when rainfall attenuation is weak or when dry period signal variability is unstable (Schleiss and Berne, 2010; Polz et al., 2020; Graf et al., 2020). The problem is more challenging in data scarce regions, where reference observations are limited and problematic links may be difficult to identify (Graf et al., 2024; Bonkoungou et al., 2025; Walraven et al., 2024).

SEVIRI CPP and PC provide independent atmospheric context that is not affected by link specific CML noise. By learning CML total loss and SEVIRI information jointly, the CNN can separate attenuation related to rainfall from non-rain signal variability more effectively. This is consistent with the improved discrimination of the satellite fusion models, which achieve higher true positive rates while keeping false positive rates low. Compared with earlier rule based uses of satellite information (van het Schip et al., 2017; Kumah et al., 2021; Graf et al., 2024), the results indicate that joint CML–SEVIRI learning is a more flexible fusion strategy.

The comparison between `CNN-TL+PC` and `CNN-WET82-PC` further supports this interpretation. Both methods use the PC product, but `CNN-WET82-PC` applies PC through a fixed rule after the CML-only CNN output, whereas `CNN-TL+PC` learns PC and CML total loss jointly inside the CNN. The higher performance of `CNN-TL+PC` therefore suggests that PC is more effective when it contributes to the learned CML–satellite representation than when it is applied as a separate threshold based constraint.

This fusion perspective also has relevance beyond CML rainfall monitoring. The main analysis shows that SEVIRI information improves CML based wet–dry classification by providing atmospheric context for ambiguous CML signal changes. The supplementary analysis in Sect. S1.3 gives the complementary perspective: satellite only CNNs using PC, CPP, or both products already contain useful rainfall information, but adding CML total loss generally improves the corresponding models. Together, these results suggest that the value of the fusion is two-way. SEVIRI helps reduce ambiguity in CML based rain detection, while CML total loss provides close to surface information that is not fully captured by geostationary satellite products alone. This makes the approach relevant not only for the CML community, but also for satellite based rainfall applications where CMLs can act as a complementary ground source.

5.2 Hydrological effect on rainfall volume

`CNN-TL` misses a large fraction of the reference rainfall volume. A CML only classifier can therefore show reasonable detection skill while still losing a substantial part of the rainfall volume. This is important because rain and dry classification is directly linked to baseline estimation in CML rainfall retrieval (Schleiss and Berne, 2010; Overeem et al., 2016). If wet periods are classified as dry, rainfall attenuation can be treated as part of the baseline and the resulting rainfall accumulation can be underestimated.

Satellite information strongly reduces this missed rainfall. The largest improvement is in the true positive rainfall contribution; the false positive rainfall contribution remains low. The satellite fusion models therefore do not improve only by becoming

https://doi.org/10.5194/egusphere-2026-3905
Preprint. Discussion started: 17 August 2026

more permissive: they recover rainfall that the CML only model classifies as dry. Previous studies showed that satellite information can reduce missed rainfall events and improve detection, especially when the CML signal alone is ambiguous (van het Schip et al., 2017; Kumah et al., 2021; Graf et al., 2024). Our rainfall contribution analysis localises the gain in terms of rainfall volume.

The improvement is most visible outside the very light rainfall range, specifically within the transitional light II class. Very light rainfall remains difficult for all models because it produces weak CML attenuation close to the noise level of the signal. The behaviour is expected for CML rainfall sensing, since short links, low rainfall rates, and limited signal resolution or quantisation steps make weak rainfall hard to detect (Messer et al., 2006; Leijnse et al., 2008; Schleiss and Berne, 2010). For the light II and stronger rainfall regimes, the satellite fusion models identify a much larger part of the rainfall volume as true positive, which matters for rainfall retrieval because missed wet periods propagate directly into underestimated rainfall accumulation.

5.3 Noisy dry periods and false wet detections

The probability analyses provide a more direct explanation of this behaviour. Compared with `CNN-TL`, the satellite based models assign lower rain probabilities during dry periods. This lowers the dry period probability baseline and reduces the number of dry samples that approach or exceed the decision threshold. The effect is especially visible during high RSTD dry periods, where the CML signal has strong short term variability but the reference radar classifies the period as dry. These conditions represent a stress case for signal only classification, because non-rain variability can resemble rainfall attenuation. The selected noisy link example and the high RSTD dry period analysis show the same pattern: `CNN-TL` gives elevated rain probabilities during difficult dry periods, while the satellite based models shift the probabilities downward. The temporal and spatial test diagnostics in Sect. S1.4 and Fig. S4 of the Supplement show the same probability pattern under a stricter test setup, providing supporting evidence for this interpretation.

The divergence between CML signal variability and the radar dry label may partly reflect spatial representativeness differences or transient localised attenuation that is not resolved by the radar grid. Individual cases therefore cannot be interpreted as unambiguous sensor artefacts. However, the same probability shift is observed systematically across dry periods: the satellite-based models assign lower rain probabilities than `CNN-TL`, especially when the CML signal is highly variable. This repeated pattern points to a model behaviour rather than a conclusion drawn from isolated radar–CML mismatches. The satellite inputs therefore appear to reduce false wet responses associated with link-specific dry signal variability, while the possibility of local reference uncertainty remains acknowledged.

This is relevant because erratic or unstable CMLs are often removed before the rain event detection step. Previous studies removed CMLs where the rolling standard deviation of the total loss exceeded a given threshold for a large part of the time (Graf et al., 2020; Blettner et al., 2023; Øydvin et al., 2024). The present results suggest that such difficult links do not always need to be treated only as noise: in some cases, useful rainfall information may still be extracted when total loss is combined with independent satellite information. This is consistent with previous work showing that SEVIRI information can improve rain event detection for CMLs that are difficult to process with signal based methods (Graf et al., 2024), and with similar

https://doi.org/10.5194/egusphere-2026-3905
Preprint. Discussion started: 17 August 2026

motivation from CML rainfall estimation in Zambia, where sparse and irregular CML networks make rainfall retrieval more challenging (Blettner et al., 2024). In this context, `CNN-TL+CPP` appears useful during dry periods with strong CML signal variability, while `CNN-TL+PC` remains competitive with a simpler satellite input.

5.4 Transfer between CML networks

Transfer between datasets is a known challenge in machine learning. Good performance on one dataset does not guarantee good performance on another when the input distribution changes. For CMLs, link length, frequency, hardware, quantisation, sampling, and local signal behaviour can differ strongly between telecommunication networks (Leijnse et al., 2008; Polz et al., 2020; Blettner et al., 2023).

The transfer experiments show that the satellite fusion models are more stable than `CNN-TL` in both transfer directions. This suggests that adding SEVIRI information can reduce the classifier's dependence on the CML signal properties of the training network. This is important because the CML signal is strongly shaped by local link characteristics, while the SEVIRI products are generated from the same satellite sensor and retrieval framework over both countries.

Transfer between the German and Czech networks is not symmetric. Czech trained models lose more performance when applied to Germany than German trained models lose when applied to Czech Republic. This asymmetry may be partly influenced by the different network property distributions described in Sect. 2.1, although it cannot be attributed to these differences alone. The Czech network covers a wider frequency range (7.45–85.75 GHz) and contains shorter path lengths (0.03–36 km), while the German dataset is concentrated below 40 GHz (10–38 GHz) and has longer path lengths (0.5–35 km). These differences may contribute to the directional transfer gap, but the result mainly shows that the training domain still matters even when satellite information is included.

A natural question is whether this transfer gap could be solved simply by using more training links from one country. The single source all link transfer setups in Sect. S1.2 and Fig. S2 of the Supplement show that this is not sufficient. Using all available links from one source dataset does not remove the transfer gap to the other dataset. This suggests that transfer depends not only on the number of training links, but also on whether the training domain represents the signal behaviour of the target network. In CML datasets, adding more links from the same source can increase the nominal dataset size without adding equivalent independent information, especially when nearby links have correlated signal levels (Overeem et al., 2011; Polz et al., 2020). This is consistent with the idea that training domain diversity contributes to transfer performance, rather than link count alone.

These results are relevant for data scarce regions, where reference data are limited and retraining a model for each local network may not be possible. A model trained only on CML total loss may learn source-network signal patterns that do not transfer well to another network. Adding SEVIRI information does not remove the need for local evaluation, but it improves transfer stability between the two tested CML networks. Future work should test this directly on longer records and on more diverse networks, including tropical and semi-arid regions.

https://doi.org/10.5194/egusphere-2026-3905
Preprint. Discussion started: 17 August 2026

5.5 Limitations

Several limitations should be considered in this work. First, the analysis is based on one month of data, which limits the seasonal generalisability of the model rankings and prevents checking long-term ranking variations. Second, some CPP microphysical variables depend on reflected solar radiation and are therefore available only during daytime, while cloud phase remains available throughout the diurnal cycle. A day–night stratification of model performance is reported in Sect. S1.1 and Fig. S1 of the Supplement and indicates similar skill in both regimes, suggesting that cloud phase together with PC carries most of the information used by the model. However, because several microphysical components are inactive at night, the stability of the model rankings across full diurnal and annual cycles still needs to be confirmed using a longer record covering more varied solar and cloud conditions. Third, the radar reference data have some spatial limitations. The RADKLIM–YW product is gauge adjusted over Germany and extends only partly into the Czech near the German border, so reference uncertainty is expected to be higher for Czech links located further from the German border. This edge uncertainty should be considered when interpreting the Czech test results.

6 Conclusions

This study evaluated CNN based wet–dry classification models that combine CML total loss with SEVIRI satellite information. The main findings are:

1. Satellite inputs improve wet–dry discrimination in both the German and Czech testing domains. The models combining CML total loss with cloud physical properties, precipitating cloud probability, or both satellite inputs outperform the CML-only CNN baseline during the study window. The comparison with the rule based PC benchmark also shows that precipitating cloud probability is more useful when it is integrated directly into the CNN than when it is applied through a separate threshold rule. Among the satellite configurations, the model combining CML total loss with precipitating cloud probability is practically attractive because it uses a simpler satellite input while performing well in most setups.

2. The rainfall contribution analysis shows that the main benefit of the satellite fusion models is a reduction in missed rainfall. The model combining CML total loss with both Cloud Physical Properties and Precipitating Cloud products gives the highest true positive rainfall fraction and the lowest false negative rainfall fraction among the tested models. The improvement is most visible outside the very light rainfall range, especially in the intermediate intensity range (1.0–$2.5\,\mathrm{mm\,h^{-1}}$). The lower rain probabilities assigned during noisy dry periods suggest that part of this improvement is linked to fewer false wet responses caused by link specific dry signal variability.

3. Transfer between the German and Czech CML networks remains asymmetric, showing that the training domain still matters and that local retraining remains preferable when reference data are available. However, the improved transfer of the satellite based models indicates that satellite inputs reduce dependence on network specific CML signal behaviour. This is relevant for data scarce regions where reference data are limited and local retraining may not be feasible.

https://doi.org/10.5194/egusphere-2026-3905
Preprint. Discussion started: 17 August 2026

4. The analysis also suggests a broader two-way value of CML–SEVIRI fusion. While the main results show that SEVIRI information improves CML based wet–dry classification, the supplementary analysis in Sect. S1.3 and Fig. S3 of the Supplement shows the complementary perspective: CML total loss can also add path integrated near-surface information to satellite based CNN rain detection. This indicates that CMLs may be useful not only as opportunistic rainfall sensors, but also as a complementary data source for satellite based rainfall applications.

Overall, the results show that SEVIRI information provides atmospheric context that improves CML based rain detection beyond a signal only CNN. The approach does not remove the need for local evaluation, but it provides a promising way to make CML rain detection less dependent on local CML signal behaviour when reference observations are limited.

Code availability. Parts of the code used in this study were adapted from the public repository: https://github.com/jpolz/cnn_cml_wet-dry_example. Additional code for data processing, model training, evaluation, and figure generation was developed by the authors. The `pycomlink` software is available at https://doi.org/10.5281/zenodo.4810169 (Chwala et al., 2024).

Data availability. The Czech CML dataset was provided by T-Mobile Czech Republic network and is subject to third-party restrictions; it is therefore not publicly available. The German CML dataset was provided by Ericsson Germany and is also not publicly available.

The RADKLIM–YW radar product is publicly available from the German Weather Service (DWD):
https://opendata.dwd.de/climate_environment/CDC/grids_germany/5_minutes/radolan/reproc/2017_002/
(last access: 28 July 2023; DWD, 2023).

The SEVIRI Cloud Physical Parameters (CPP) from the CLAAS-3 dataset are available via EUMETSAT CM SAF: https://www.cmsaf.eu.

The Precipitating Cloud (PC) product used in this study was provided by Christian Chwala. The PC and PC-Ph products are developed within the NWC SAF framework. Near-real-time data are available at:
https://www.nwcsaf.org/web/guest/nwc/geo-geostationary-near-real-time-v2021
(last access: 20 December 2023). Long-term datasets must be requested directly from NWC SAF (contact: `safnwchd@aemet.es`).

Supplement. The Supplement contains additional analyses supporting the main results, including day–night sensitivity of CPP-based models, additional transfer experiments, satellite-only and CML–SEVIRI fusion experiments, and temporal and spatial test diagnostics.

Author contributions. TS developed the methodology, processed the datasets, implemented the CNN models, performed the analysis, prepared the figures, and wrote the original draft. MF and VB supervised the study, contributed to the conceptual design, interpreted the results, and revised the manuscript. CC contributed to the CML data interpretation, methodological discussion, and manuscript revision. All authors reviewed and approved the final manuscript.

https://doi.org/10.5194/egusphere-2026-3905
Preprint. Discussion started: 17 August 2026

Competing interests. The authors declare that they have no conflict of interest.

Financial support. This work was supported by the Czech Science Foundation (GACR), Czech Republic, under Grant No. 24-13677L (MERGOSAT).

Acknowledgements. The authors thank T-Mobile operators for providing the Czech CML dataset and Ericsson Germany for providing the German CML data.

We gratefully acknowledge Christian Chwala for sharing the Precipitating Cloud (PC) product and for providing code related to the CNN-WET82-PC method following Graf et al (2024).

The RADKLIM–YW dataset was provided by the German Weather Service (DWD), and we acknowledge their open data policy.

Parts of this work build upon open-source contributions from the community, including the CNN wet–dry classification example by Polz et al (2020).

This work was also supported by the Ministry of Education, Youth and Sports of Czech Republic through the e-INFRA CZ (ID:90254).

The authors also acknowledge helpful discussions within the MERGOSAT project.

References

Bárdossy, A. and Anwar, F.: Why do our rainfall–runoff models keep underestimating the peak flows?, Hydrology and Earth System Sciences, 27, 1987–2000, https://doi.org/10.5194/hess-27-1987-2023, 2023.

Bartels, H., Weigl, E., Reich, T., Lang, P., Wagner, A., and Kohler, O.: Routineverfahren zur Online-Aneichung der Radarniederschlagsdaten mit Hilfe von automatischen Bodenniederschlagsstationen, Tech. Rep. Projekt RADOLAN, Abschlussbericht, Deutscher Wetterdienst (DWD), Offenbach am Main, Germany, in German, 2004.

Blettner, N., Fencl, M., Bareš, V., Kunstmann, H., and Chwala, C.: Transboundary Rainfall Estimation Using Commercial Microwave Links, Earth and Space Science, 10, e2023EA002 869, https://doi.org/10.1029/2023EA002869, 2023.

Blettner, N., Wiegels, R., Kunstmann, H., and Chwala, C.: Using commercial microwave links and SEVIRI observations for rainfall estimation in Zambia, EGU General Assembly 2024, Vienna, Austria, 14–19 April 2024, EGU24-10338, https://doi.org/10.5194/egusphere-egu24-10338, 2024.

Bonkoungou, J. R., Djibo, M., Doumounia, A., Ouédraogo, B. W. Y. S., Sanou, R. S., Sawadogo, M., Koalaga, Z., and Zougmoré, F.: Multi-source estimation of rainfall using opportunistic sensors in urban areas in Burkina Faso, Water Science and Technology, 92, 1412–1425, https://doi.org/10.2166/wst.2025.160, 2025.

Bruni, G., Reinoso, R., van de Giesen, N. C., Clemens, F. H. L. R., and ten Veldhuis, J. A. E.: On the sensitivity of urban hydrodynamic modelling to rainfall spatial and temporal resolution, Hydrology and Earth System Sciences, 19, 691–709, https://doi.org/10.5194/hess-19-691-2015, 2015.

Chwala, C., Gmeiner, A., Qiu, W., Hipp, S., Nienaber, D., Siart, U., Eibert, T., Pohl, M., Seltmann, J., Fritz, J., and Kunstmann, H.: Precipitation observation using microwave backhaul links in the alpine and pre-alpine region of Southern Germany, Hydrology and Earth System Sciences, 16, 2647–2661, https://doi.org/10.5194/hess-16-2647-2012, 2012.

Chwala, C., Graf, M., Polz, J., Blettner, N., and Øydvin, E.: pycomlink: Python tools for CML data processing, https://doi.org/10.5281/zenodo.4810169, 2024.

Chwala, C., Overeem, A., Øydvin, E., Petersson Wårdh, L., Seidel, J., Graf, M., Walraven, B., Covi, E., Habi, H. V., Fencl, M., de Vos, L., Giannetti, F., Green, A., O'Hara, T., Blettner, N., Keel, T., Schutz, G., El Hachem, A., Illich, N., Polz, J., Shit, T., Kaleta, L., Zulkarnaen, D., and Bareš, V.: Open-source tools for processing opportunistic rainfall sensor data: An overview of existing tools and the new OpenSense software packages poligrain, pypwsqc and mergeplg, EGUsphere, pp. 1–31, https://doi.org/10.5194/egusphere-2025-5438, preprint, 2026.

Dong, J., Crow, W. T., and Reichle, R. H.: Improving Rain/No-Rain Detection Skill by Merging Precipitation Estimates from Different Sources, Journal of Hydrometeorology, 21, 2419–2429, https://doi.org/10.1175/JHM-D-20-0097.1, 2020.

EUMETSAT: Meteosat Second Generation (MSG) Level 1.5 Image Data Format Description, https://www.eumetsat.int, sEVIRI instrument and data characteristics, 2017.

Fawcett, T.: An introduction to ROC analysis, Pattern Recognition Letters, 27, 861–874, https://doi.org/10.1016/j.patrec.2005.10.010, 2006.

Graf, M., Chwala, C., Polz, J., and Kunstmann, H.: Rainfall estimation from a German-wide commercial microwave link network: optimized processing and validation for 1 year of data, Hydrology and Earth System Sciences, 24, 2931–2950, https://doi.org/10.5194/hess-24-2931-2020, 2020.

Graf, M., Wagner, A., Polz, J., Lliso, L., Lahuerta, J. A., Kunstmann, H., and Chwala, C.: Improved rain event detection in commercial microwave link time series via combination with MSG SEVIRI data, Atmospheric Measurement Techniques, 17, 2165–2182, https://doi.org/10.5194/amt-17-2165-2024, 2024.

Habi, H. V. and Messer, H.: Wet-Dry Classification Using LSTM and Commercial Microwave Links, in: 2018 IEEE 10th Sensor Array and Multichannel Signal Processing Workshop (SAM), pp. 149–153, https://doi.org/10.1109/SAM.2018.8448679, 2018.

International Telecommunication Union: Specific attenuation model for rain for use in prediction methods, Recommendation itu-r p.838-3, International Telecommunication Union, Geneva, Switzerland, https://www.itu.int/rec/R-REC-P.838-3-200503-I/en, 2005.

Kamtchoum, E. V., Nzeukou Takougang, A. C., and Tayou Djamegni, C.: A Machine Learning Approach for the Classification of Wet and Dry Periods Using Commercial Microwave Link Data, SN Computer Science, 3, 227, https://doi.org/10.1007/s42979-022-01143-8, 2022.

Kumah, K. K., Hoedjes, J. C. B., David, N., Maathuis, B. H. P., Gao, H. O., and Su, Z.: The MSG Technique: Improving Commercial Microwave Link Rainfall Intensity by Using Rain Area Detection from Meteosat Second Generation, Remote Sensing, 13, 3274, https://doi.org/10.3390/rs13163274, 2021.

Leijnse, H., Uijlenhoet, R., and Stricker, J. N. M.: Microwave Link Rainfall Estimation: Effects of Link Length and Frequency, Temporal Sampling, Power Resolution, and Wet Antenna Attenuation, Advances in Water Resources, 31, 1481–1493, https://doi.org/10.1016/j.advwatres.2008.03.004, 2008.

Meirink, J. F., Karlsson, K.-G., Solodovnik, I., Hüser, I., Benas, N., Johansson, E., Håkansson, N., Stengel, M., Selbach, N., Schröder, M., and Hollmann, R.: CLAAS-3: CM SAF CLoud property dAtAset using SEVIRI – Edition 3, https://doi.org/10.5676/EUM_SAF_CM/CLAAS/V003, 2022.

Messer, H., Zinevich, A., and Alpert, P.: Environmental monitoring by wireless communication networks, Science, 312, 713, https://doi.org/10.1126/science.1120034, 2006.

Miao, C., Gou, J., Hu, J., and Duan, Q.: Impacts of Different Satellite-Based Precipitation Signature Errors on Hydrological Modeling Performance Across China, Earth's Future, 12, e2024EF004 954, https://doi.org/10.1029/2024EF004954, 2024.

Overeem, A., Leijnse, H., and Uijlenhoet, R.: Measuring urban rainfall using microwave links from commercial cellular communication networks, Water Resources Research, 47, W12 505, https://doi.org/10.1029/2010WR010350, 2011.

Overeem, A., Leijnse, H., and Uijlenhoet, R.: Country-wide rainfall maps from cellular communication networks, Proceedings of the National Academy of Sciences, 110, 2741–2745, https://doi.org/10.1073/pnas.1217961110, 2013.

Overeem, A., Leijnse, H., and Uijlenhoet, R.: Retrieval algorithm for rainfall mapping from microwave links in a cellular communication network, Atmospheric Measurement Techniques, 9, 2425–2444, https://doi.org/10.5194/amt-9-2425-2016, 2016.

Overeem, A., Leijnse, H., van der Schrier, G., van den Besselaar, E., Garcia-Marti, I., and de Vos, L. W.: Merging with crowdsourced rain gauge data improves pan-European radar precipitation estimates, Hydrology and Earth System Sciences, 28, 649–668, https://doi.org/10.5194/hess-28-649-2024, 2024.

Øydvin, E., Graf, M., Chwala, C., Wolff, M. A., Kitterød, N.-O., and Nilsen, V.: Technical note: A simple feedforward artificial neural network for high-temporal-resolution rain event detection using signal attenuation from commercial microwave links, Hydrology and Earth System Sciences, 28, 5163–5171, https://doi.org/10.5194/hess-28-5163-2024, 2024.

Polz, J., Chwala, C., Graf, M., and Kunstmann, H.: Rain event detection in commercial microwave link attenuation data using convolutional neural networks, Atmospheric Measurement Techniques, 13, 3835–3853, https://doi.org/10.5194/amt-13-3835-2020, 2020.

Pudashine, J., Guyot, A., Petitjean, F., Pauwels, V. R. N., Uijlenhoet, R., Seed, A., Prakash, M., and Walker, J. P.: Deep Learning for an Improved Prediction of Rainfall Retrievals From Commercial Microwave Links, Water Resources Research, 56, e2019WR026 255, https://doi.org/10.1029/2019WR026255, 2020.

https://doi.org/10.5194/egusphere-2026-3905
Preprint. Discussion started: 17 August 2026

Rombeek, N., de Vos, L. W., Overeem, A., Leijnse, H., and Uijlenhoet, R.: Evaluation of high-intensity rainfall observations from personal weather stations, rain gauges, and weather radar, Hydrology and Earth System Sciences, 29, 4585–4605, https://doi.org/10.5194/hess-29-4585-2025, 2025.

Schleiss, M. and Berne, A.: Identification of dry and rainy periods using telecommunication microwave links, IEEE Geoscience and Remote Sensing Letters, 7, 611–615, https://doi.org/10.1109/LGRS.2010.2043052, 2010.

Tobin, K. J. and Bennett, M. E.: Adjusting Satellite Precipitation Data to Facilitate Hydrologic Modeling, Journal of Hydrometeorology, 11, 966–978, https://doi.org/10.1175/2010JHM1206.1, 2010.

van het Schip, T. I., Overeem, A., Leijnse, H., Uijlenhoet, R., Meirink, J. F., and van Delden, A. J.: Rainfall measurement using cell phone links: classification of wet and dry periods using geostationary satellites, Hydrological Sciences Journal, 62, 1343–1353, https://doi.org/10.1080/02626667.2017.1329588, 2017.

Walraven, B., Overeem, A., Coenders-Gerrits, M., Hut, R., van der Valk, L., and Uijlenhoet, R.: Relating Rainfall Retrieval Parameters to Network and Environmental Features to Improve Rainfall Estimates from Commercial Microwave Links in the Tropics, Journal of Hydrometeorology, 25, 1769–1791, https://doi.org/10.1175/JHM-D-24-0023.1, 2024.

Winterrath, T., Rosenow, W., and Weigl, E.: On the DWD quantitative precipitation analysis and nowcasting system for real-time application in German flood risk management, IAHS Publication, 351, 323–330, 2012.

Winterrath, T., Brendel, C., Hafer, M., Junghänel, T., Kothe, S., Lengfeld, K., Quirmbach, M., and Walawender, E.: RADKLIM Version 2017.002: Reprocessed Gauge-Adjusted Radar Data for Germany, Tech. Rep. Berichte des Deutschen Wetterdienstes 250, Deutscher Wetterdienst (DWD), Offenbach am Main, Germany, https://doi.org/10.5676/DWD/RADKLIM_YW_V2017.002, 2018.

Zambrano-Bigiarini, M., Nauditt, A., Birkel, C., Verbist, K., and Ribbe, L.: Temporal and spatial evaluation of satellite-based rainfall estimates across the complex topographical and climatic gradients of Chile, Hydrology and Earth System Sciences, 21, 1295–1320, https://doi.org/10.5194/hess-21-1295-2017, 2017.